EUROPEAN JOURNAL OF CANCER 47 (2011) 640–648

available at www.sciencedirect.com

ScienceDirect

journal homepage: www.ejconline.com

The acridone derivative MBLI-87 sensitizes breast cancer resistance protein-expressing xenografts to irinotecan

O. Arnaud [d], A. Boumendjel [c], A. Gèze [c], M. Honorat [a,b], E.L. Matera [b], J. Guitton [a,f], W.D. Stein [e], S.E. Bates [e], P. Falson [d], C. Dumontet [a,b], A. Di Pietro [d], L. Payen [a,b,g,*]

[a] ISPB, Université Lyon 1, 69008 Lyon, France
[b] Inserm U590, Centre Léon Bérard, FNCLCC, 69008, France
[c] Département de Pharmacochimie Moléculaire, UMR 5063, CNRS/Université de Grenoble, 38041 Grenoble Cedex 9, France
[d] Equipe labellisée Ligue 2009, Institut de Biologie et Chimie des Protéines, UMR 5086 CNRS/Université Lyon 1, IFR 128 BioSciences Gerland-Lyon Sud, 69367 Lyon Cedex 07, France
[e] Medical Oncology Branch, Center for Cancer Research, National Institutes of Health, Bethesda, MD 20892, USA
[f] Hospices Civils de Lyon, Centre Hospitalier Lyon-Sud, Laboratoire de Ciblage Thérapeutique en Cancérologie, 69495 Pierre-Bénite, France
[g] Hospices Civils de Lyon, Centre Hospitalier Lyon-Sud, Laboratoire de biochimie, 69495 Pierre-Bénite, France

ARTICLE INFO

Article history:
Received 29 September 2010
Received in revised form 15 November 2010
Accepted 23 November 2010
Available online 7 January 2011

Keywords:
ABC transporter
ABCG2
Irinotecan
Multidrug resistance
Reversion

ABSTRACT

The breast cancer resistance protein ABCG2 confers cellular resistance to irinotecan (CPT-11) and its active metabolite SN-38. We utilised ABCG2-expressing xenografts as a model to evaluate the ability of a non-toxic ABCG2 inhibitor to increase intracellular drug accumulation. We assessed the activity of irinotecan *in vivo* in SCID mice: irinotecan completely inhibited the development of control pcDNA3.1 xenografts, whilst only delaying the growth of ABCG2-expressing xenografts. Addition of MBLI-87, an acridone derivative inhibitor, significantly increased the irinotecan effect against the growth of ABCG2-expressing xenografts. *In vitro*, MBLI-87 was as potent as GF120918 against ABCG2-mediated irinotecan efflux, and additionally was specific for ABCG2. A significant sensitisation to irinotecan was achieved despite the fact that doses remained well below the maximum tolerated dose (due to the rather limited solubility of MBLI-87). This suggested that MBLI-87 is an excellent candidate to prevent drug efflux by ABCG2, without altering plasma concentrations of irinotecan and SN-38 after IP (intra-peritoneal) injections. This could constitute a useful strategy to improve drug pharmacology, to facilitate drug penetration into normal tissue compartments protected by ABCG2, and potentially to reverse drug resistance in cancer cells.

1. Introduction

Multidrug efflux pumps from the ATP-binding cassette (ABC) family are thought to play important roles in drug absorption and distribution, normal tissue protection and, perhaps, anticancer drug-resistance. Although efforts to reverse drug resistance using ABCB1/P-glycoprotein (Pgp) inhibitors essentially failed in the past, it is not known whether this was because the target was not as prevalent as was previously thought or was due to inadequate inhibition or the concurrent expression of other transporters able to compensate for the inhibition of Pgp. The question of whether inhibitors of other ABC transporters could be exploited clinically has rarely been addressed. Since a number of the targeted anticancer agents have been found to be substrates or modulators of multidrug efflux pumps, it has become important to define their possible

* *Corresponding author*: Address: Inserm U590, 8, Avenue Rockefeller, 69008 Lyon, France. Tel.: +33478777236; fax: +33478777088.
E-mail address: Lea.payen@recherche.univ-lyon1.fr (L. Payen).
0959-8049/$ - see front matter
doi:10.1016/j.ejca.2010.11.019

role in multidrug resistance. Furthermore, inhibition of the multidrug efflux pumps has potential utility beyond reversal of resistance, for instance, in improving the delivery of substrate drugs to the central nervous system (CNS).[1–3] For example, it was recently reported that CNS penetration of lapatinib in animal models is limited by both Pgp and ABCG2.[4] Our strategy is to use reversal of drug resistance in xenografts as a proof of the concept that improved drug delivery and accumulation, through inhibition of efflux pumps, can indeed be achieved *in vivo*. HEK293 human embryonic kidney cells were previously shown to be able to grow as xenografts in SCID mice.[4] This offered the possibility of a defined model system of transfected cells in which ABCG2 would be the only difference from control xenografts, and that levels would not be too high, in contrast to other model systems in which drug selection had been utilised to achieve ABCG2 up-regulation. This would lay the groundwork for re-testing the hypothesis that ABC transporters contribute to drug resistance and that their inhibition could prove useful in patients for targeting ABC transporters that prevent drug accumulation in the CNS or for improving and normalising oral drug bioavailability.

ABCG2, also termed breast cancer resistance protein or BCRP, is an important ABC half-transporter. It effluxes a wide range of substrates, including natural compounds such as porphyrins and anticancer drugs such as mitoxantrone, irinotecan (CPT-11)[5] and SN-38, its pharmacologically-active metabolite, thus overlapping the substrate spectra of ABCB1 and ABCC1.[6] A few potent inhibitors have been described, including GF120918, tariquidar, Ko143 – a derivative of fumitremorgin C (a highly toxic tremorgenic mycotoxin isolated from *Aspergillus fumigatus*), imatinib and gefitinib (GEFI, ZD1839, Iressa).[7] The latter compound is an efficient tyrosine-kinase inhibitor targeting the epidermal growth factor receptor (EGFR) and used in lung cancer clinical trials.[8,9] Controversial data have been reported about its transport by ABCG2.[9,10] This is apparently due to the fact that gefitinib is a substrate at low concentrations whereas inhibitory properties are observed *in vivo* at higher concentrations.[11,12] Nevertheless, high and maximum tolerated doses of gefitinib (over 75 mg/kg) have demonstrated ability to reverse the SN-38-dependent resistant phenotype.[10,12,13] The requirement for such high gefitinib doses would obviously constitute serious limitations for ABCG2 modulation in a clinical setting. New ABCG2 inhibitors have been recently designed and optimised amongst flavonoids, based on flavone[14] and acridone[15] derivatives. One acridone, MBLI-87, also called acridone 4b, was found to be as potent *in vitro* as GF120918 against ABCG2-mediated mitoxantrone efflux,[15] with the advantage of not inhibiting ABCB1 and ABCC1.[16] To further characterise MBLI-87 effects against ABCG2 transport activity, we evaluated its *in vitro* inhibition of irinotecan efflux and its *in vivo* modulatory effect on ABCG2-related drug resistance in xenografts.

2. Material and methods

2.1. Cell cultures

The two HEK293 cell models used, transfected with either wild-type ABCG2 or empty pcDNA3.1 vector,[17] were cultured as described.[14]

2.2. Animal studies

SCID mice (Charles River Laboratories) were handled in accordance with the Guide for the Care and Use of Laboratory Animals, and all procedures followed protocols approved by the Animal Facility veterinarian board. Eight week-old female mice were subcutaneously inoculated with either pcDNA3.1- or ABCG2-HEK293 cells (8.2×10^6 in 100 μL DMEM medium and matrigel solution (50% v/v)/inoculation). Since pcDNA3.1- and ABCG2-xenografts responded differently to irinotecan therapy, each mouse was implanted on the left and right flanks with the same tumour cell type. All mice implanted with ABCG2-xenografts were randomised within eight groups. Similar procedures were carried out for control (pcDNA3.1) xenografted mice. After randomisation, each mouse was independently identified by a colour code. Tumour volume was determined, in mm^3, by measuring tumour length (l) and width (w), and using the formula: volume = $(4 * 3.14((l + w)/2)^3)/3$. Time zero was the day of cell inoculation. Xenograft tumours were harvested when their volume reached approximately 1800 mm^3.

2.3. Drug formulation and administration

MBLI-87, which was not soluble in either water or saline vehicles, was formulated in enzymatically modified cyclodextrin-based colloidal suspension by the solvent displacement method.[19] An organic phase containing acetone (30 mL), (γCD-C10 at 2 mg/mL),[18,19] benzyl benzoate (600 μL), a lipophilic surfactant Montane® 80 (8 mg/mL) and the drug (9 mg) was added into 60 mL of glucose (3.6% w/w) supplemented with the hydrophilic surfactant Montanox® 80 (4 mg/mL) under magnetic stirring (500 rpm) at 25 °C. The obtained organo-aqueous suspension was submitted to reduced pressure in order to eliminate acetone and the aqueous suspension volume was adjusted to reach isotonicity. The suspensions were filtered through 0.45 μm and stored in sterile glass vials (10 mL) for further *in vivo* studies. The nanoparticle size, measured by quasi-elastic light scattering, was around 185–195 nm (PI 0.05).[20] The MBLI-87 concentration recovered in the suspension (0.16 mg/mL) was assayed spectrophotometrically at 393 nm in ethanol after dissolution of a known volume of suspension in the organic solvent. The drug fraction solubilised in the aqueous phase of the suspension was evaluated after separation of the nanoparticles from supernatant by ultracentrifugation (300,000*g*, 1.5 h, 20 °C) and was in agreement with the poor MBLI-87 aqueous solubility (0.007 mg/mL at 25 °C). In the final suspension, 95% of the drug amount recovered was associated with the nanoparticles. The stability studies indicated that the characteristics of MBLI-87-loaded nanoparticle suspensions remained unchanged in terms of mean size particles and drug concentration during at least 2 months. Thus, the same batch of colloidal suspension could be used repeatedly.

The suspension of MBLI-87-loaded nanoparticles (later called MBLI-87), at 0.16 mg/mL, was administered by intraperitoneal (IP) injection as a 2.4 mg/kg dose, 5 days/week on two consecutive weeks followed by a 14-day rest period. Unloaded colloidal suspension (without MBLI-87) was called NANO (MBLI-87 vehicle). Irinotecan, kindly provided by

Dr. Hamedi-Sangsari (MAP-France company), was administered by IP injection at 30 mg/kg (0.1 mL water), 3 days/week on two consecutive weeks followed by a 14-day rest period. Tumour-bearing SCID mice were randomised into eight groups the day after cell implantation, before receiving drugs. The two-week period of drug administration plus its 14-day rest constituted one therapy cycle; mice thus received 2 cycles over 8 weeks.

2.4. Western blot analysis

Xenografts were resuspended in a hypotonic buffer (5 mM EDTA, 10 mM Tris/HCl pH 8, 10 mM KCl, protease inhibitor cocktail) in an ice-cold Dounce homogeniser for 1 h before homogenisation 30 times on ice. After centrifugation (15 min, 1000*g*), supernatants were collected, and protein content quantified using the bicinchoninic acid assay (provided by Sigma–Aldrich, Inc.). 10 μg of proteins were separated by 10% (w/v) SDS–polyacrylamide gel electrophoresis. PVDF membranes were probed with the anti-ABCG2 monoclonal antibody BXP-21 (1/200, Tebu-bio), and a polyclonal alpha-tubulin antibody (1/500, Sigma). ABCG2 was detected using the Enhanced Chemiluminescence Plus detection kit (Amersham Pharmacia Biotech), and densitometry performed using QuantityOne® software.

2.5. In vitro and in vivo quantification of irinotecan and SN-38

For *in vitro* experiments, cells were first plated at 750,000 cells/well in 6-well plates. They were loaded with 2 μM irinotecan in DMEM medium (without FBS) for 60 min at 37 °C in the absence or presence of either 5 μM GF120418, 5 μM MBLI-87 or 10 μM fumitremorgin C. During the uptake period, irinotecan could be metabolised into SN-38. After two washings with ice-cold PBS (to inhibit active efflux capabilities), cells were collected in 1 mL of ice-cold PBS, submitted to centrifugation (5 min at 1500*g*) and lysed by 500 μL pure methanol. Finally, intracellular irinotecan accumulation was quantified in a cell aliquot by HPLC MS/MS, according the analytical description below. Specific transitions for SN-38, APC and SN-38G were also monitored in order to assess potential metabolism of irinotecan in the cells. We were unable to detect APC and SN-38G under our experimental conditions. Results (expressed in ng irinotecan/mg protein) were normalised to cellular protein content (Bradford assay).

For *in vivo* experiments, irinotecan disposition was evaluated in tumour-free SCID mice after a single MBLI-87 (3.45 mg/kg) and/or irinotecan (20 mg/kg) IP administration (injection route used in *in vivo* protocol). Approximately 1 mL of blood was collected with heparinised syringes (5 animals per time point) at 0.5, 1, 3, 6, or 24 h after injection. Plasma fractions were extracted from each blood sample by centrifugation (5 min, 5000*g*).

For analytical quantification, irinotecan and SN-38 were kindly furnished by Pfizer (Kalamazoo, USA) and camptothecin was obtained from Sigma (Saint-Quentin Fallavier, France). For plasma samples, the preparation was carried out according to the following procedure: 50 μL of plasma, 20 μL of internal standard (camptothecin at 1 μg/mL) and 300 μL of formic acid (2% v/v) were mixed vigorously for 10 s. The mixture was applied to previously conditioned SPE extraction cartridges (Oasis© HLB 30 mg – Waters, Milford, USA). The cartridge was washed with 1 mL of a mixture of methanol and 2% formic acid (20/80, v/v) and the elution was then carried out with 1 mL of methanol. The eluate was evaporated to dryness under a stream of nitrogen, and the residue was resuspended in 100 μL of mobile phase. For cell samples, following the incubation period with irinotecan, the cells were washed three times with ice-cold PBS and then 300 μL of methanol were added and samples were stored at −20 °C in this condition. The sample preparation was performed by adding 20 μL of camptothecin (internal standard) at 1 μg/mL, and then samples were mixed and centrifuged at 12,000*g* for 5 min at 10 °C. The supernatant was removed and evaporated to dryness under a stream of nitrogen. The residues were resuspended in 300 μL of mobile phase.

For plasma and cell incubation samples, the solution was then transferred to a glass vial kept at 10 °C in the autosampler and 10 μL was injected in the HPLC device. Irinotecan and SN-38 were separated on a Hypersil Gold 100 mm × 2.1 mm column (ThermoFisher, San Jose, USA). The separation was performed using a gradient mode with a mobile phase constituted by water and acetonitrile, both solutions containing acetic acid at 0.1%. The mobile phase was delivered through the column (temperature maintained at +30 °C) at a flow rate of 200 μL/min. The detection was carried out with a Quantum-Ultra (ThermoFisher, San Jose, USA) triple quadrupole mass spectrometer. The instrument was operated in positive ion mode with electrospray (ESI) source. The quantification was performed using the transitions *m/z* 587 → 124 (irinotecan), *m/z* 393 → 349 (SN-38) and *m/z* 349 → *m/z* 305 (camptothecin).

Calibration curves were constructed by plotting the ion abundance peak area ratio irinotecan/camptothecin and SN-38/camptothecin as function of irinotecan or SN-38 plasma concentration. Calibration curves were tested from 5 to 1000 ng/mL and from 0.5 to 100 ng/mL for irinotecan and SN-38, respectively. For both compounds, a weighting factor (1/concentration) was applied and a mean least-squares linear regression correlation coefficient of greater than 0.995 was obtained. The concentrations back-calculated from the equation of the regression analysis were lower than 8.5% for precision and than 5% for accuracy for both compounds. The within-run and between-run variability (precision) and the mean predicted concentration (accuracy) were analysed at three different concentrations (0.5, 5 and 55 ng/mL for SN-38 and 7, 70 and 750 ng/mL for irinotecan) in sextuplicate on four separate days and were lower than 10% except for SN-38 at 0.5 ng/mL, with a between-run variability equal to 12.8%. All parameters fulfilled the respective requirements of the Washington consensus conference on analytical methods validation.

2.6. Statistical analysis

Irinotecan accumulation histograms (Fig. 1) were constructed with Excel, and expressed as mean ± SD. The statistical analyses (unilateral *t*-test) were performed with Excel. Growth curves were constructed with Excel as a plot of tumour

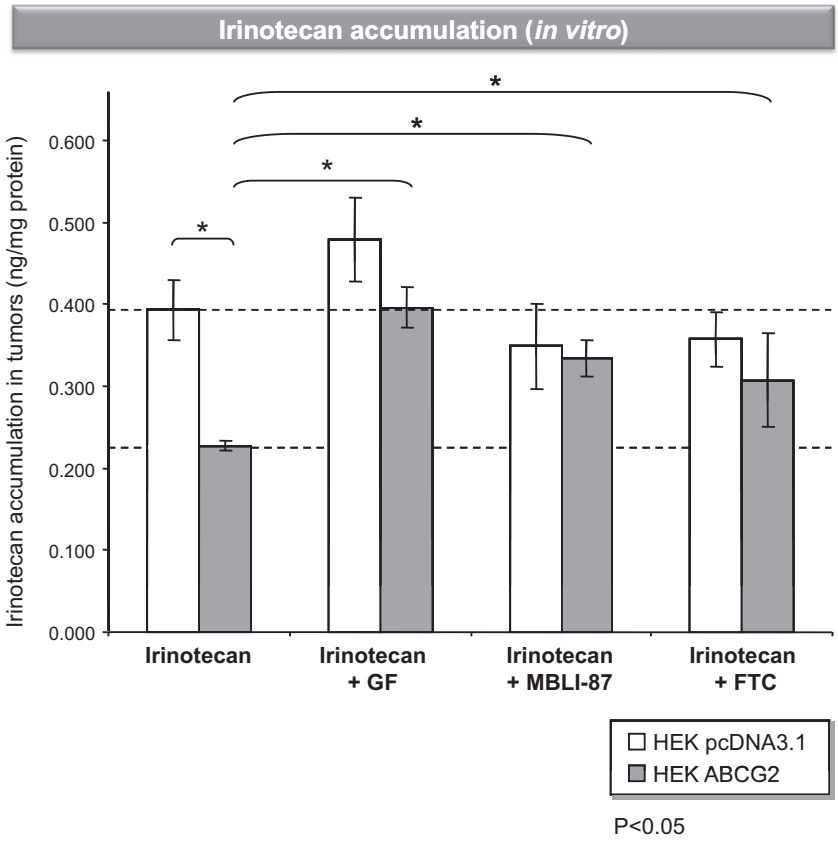

Fig. 1 – *In vitro* irinotecan accumulation in control and ABCG2-expressing cells. Cells were loaded with 2 μM irinotecan in DMEM medium (without FBS) for 60 min at 37 °C in the absence or presence of either 5 μM GF120418, 5 μM MBLI-87 or 10 μM fumitremorgin C. Intracellular irinotecan accumulation was quantified by HPLC MS/MS. Results were expressed as ng irinotecan/mg protein.

volume ± SE against time. In Fig. 3A and B, statistical evaluation was carried out with the non-parametric Mann Whitney test. In Fig. 3C and Table 1, growth curves were constructed with SigmaPlot® (Systat Software, San Jose, CA), by analysing data as a plot of tumour volume ± SE against time, and the statistical analyses (paired *t*-test) were performed with Sigmastat® (Systat Software).

3. Results and discussion

To compare the *in vitro* effects of MBLI-87 on irinotecan accumulation in both control pcDNA3.1-HEK293 cells and ABCG2-expressing HEK293 cells, the two cell lines were incubated for 60 min with 2 μM irinotecan in the absence or presence of either 5 μM MBLI-87, 5 μM GF120918 or 10 μM fumitremorgin C (Fig. 1). Then, cellular accumulation of irinotecan was quantified by HPLC MS/MS. This demonstrated that irinotecan was approximately 1.7-fold less accumulated in ABCG2-expressing HEK293 cells than in control cells. In ABCG2-HEK293 cells, irinotecan accumulation was increased by co-exposure to any ABCG2 modulator (10 μM fumitremorgin C, 5 μM GF120918 or 5 μM MBLI-87), whilst these modulators had no effect in the control cells (Fig. 1). This demonstrated that MBLI-87 is indeed a potent inhibitor of ABCG2, increasing irinotecan cellular accumulation.

We have used pcDNA3.1 and ABCG2 stable transfectants in HEK293 cells as a cellular tool[17] to characterise both *in vitro* and *in vivo* effects of ABCG2 modulators. In contrast to drug-selected ABCG2 cancer cells, these models allow access to a true negative control (here the empty pcDNA3.1 transfected cell line) in order to validate the specificity, and to exactly evaluate the net effect of our inhibitor on the ABCG2 target. We first confirmed the previously reported tumourigenicity of HEK293 cells[21] and then determined the optimal concentration range of MBLI-87 and irinotecan, non-toxic doses in combination and the schedule of their administration to SCID mice over the 8-week protocol. We characterised the maximum tolerated doses of irinotecan (30 mg/kg for 3 days/week) in combination with either control NANO (300 μL for 5 days/week) or MBLI-87 (2.4 mg/kg in 300 μL NANO for 5 days/week). Higher doses of irinotecan were not used as they resulted in loss of weight and modifications in behaviour, both defined as reference elements by the Animal Facility veterinarian board to *in vivo* quantify the toxicity of the molecules. No difference in toxicity was observed according to the treatments.

MBLI-87 could not be solubilised in oil, saline or water vehicles. The chronic administration schedule of 50 μL pure DMSO was not recommended by the ethics committee of our institution, as described in the Section 2. We used a

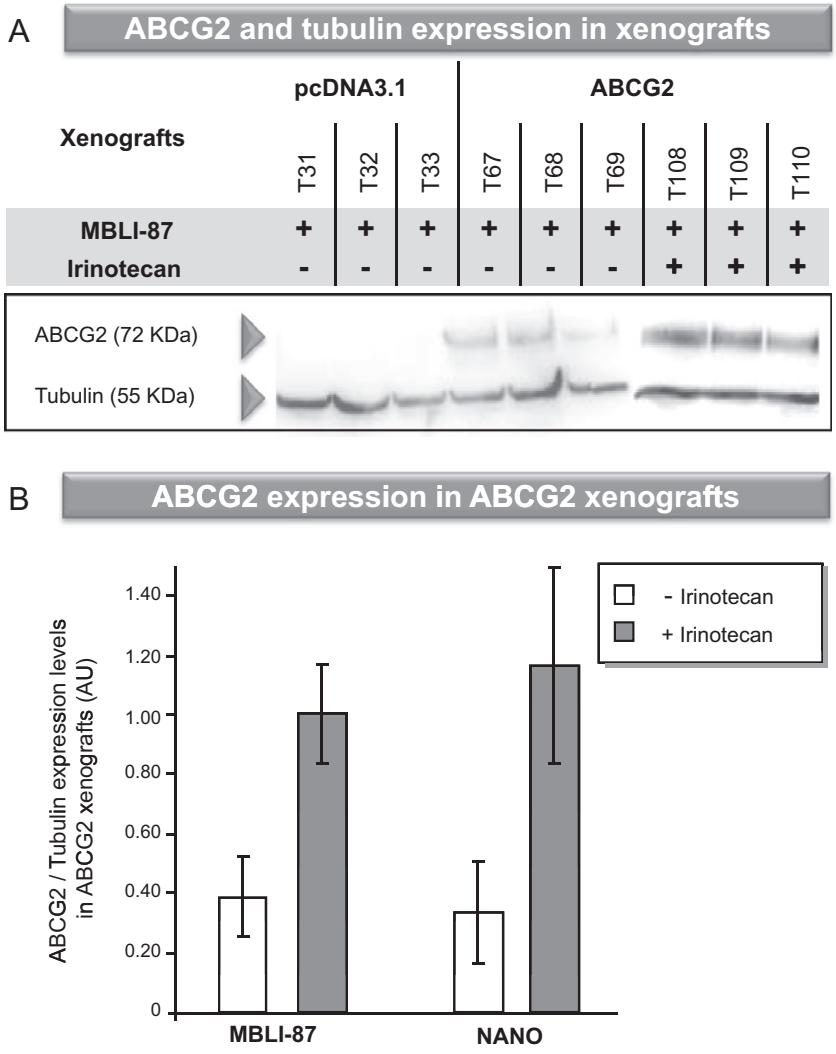

Fig. 2 – (A) ABCG2 expression in xenografts. As soon as the tumour volume reached approximately 1800 mm^3, mice were sacrificed, and crude membrane fractions were prepared from (T31–T110) individual xenografts. ABCG2 expression was quantified by immunoblotting with the monoclonal BXP21 antibody, as described in Section 2. (B) Effects of treatment with irinotecan and/or MBLI-87 on ABCG2 expression levels. ABCG2 expression was quantified as in A, and normalised to the alpha-tubulin content (ABCG2 expression levels/tubulin expression levels). Protein level ratios were expressed as arbitrary units (AU). The values are means ± S.E.

specific and complex formulation in nanoparticles (NANO) to allow its administration to mice. Consequently, for evaluating the net MBLI-87 effect on the growth of ABCG2-expressing xenografts, we carried out control conditions with the nanoparticles alone (NANO). When the tumour volume reached approximately 1800 mm^3, mice were sacrificed and xenografts harvested. ABCG2 expression levels were quantified by Western blot analysis and, as expected, the ABCG2 protein was only detected in ABCG2 xenografts (Fig. 2A). Since control (pcDNA3.1) tumours did not grow during the first 60 days, we did not check any irinotecan effect on ABCG2 expression. We did not find any statistical effect of NANO vehicle on the growth curves of either pcDNA3.1 HEK 293 cells or ABCG2 HEK 293 cells (data not shown). NANO did not significantly alter the effect of irinotecan on the growth of ABCG2 xenografts (data not shown). Interestingly, irinotecan treatment, whether combined with MBLI-87 or under control conditions (NANO), resulted in higher ABCG2 expression in xenografts (Fig. 2A and B), whereas MBLI-87 alone had no effect (Fig. 2B). This strongly suggested that the anticancer agent irinotecan selected ABCG2-expressing cells having high efflux capability, which then could limit irinotecan chemotherapeutic activity or disposition.

We next evaluated MBLI-87 circumvention of *in vivo* drug resistance by submitting mice to two chemotherapy cycles, administering irinotecan (30 mg/kg for 3 days/week) in combination with either control NANO (300 μL for 5 days/week) or MBLI-87 (2.4 mg/kg in 300 μL NANO for 5 days/week), the day after cell implantation. The first drug therapy period (from day 1 to 15) avoided physical variability of irinotecan distribution in xenografts (since tumours were small and not completely established in 3-D tissue). This first chemo-

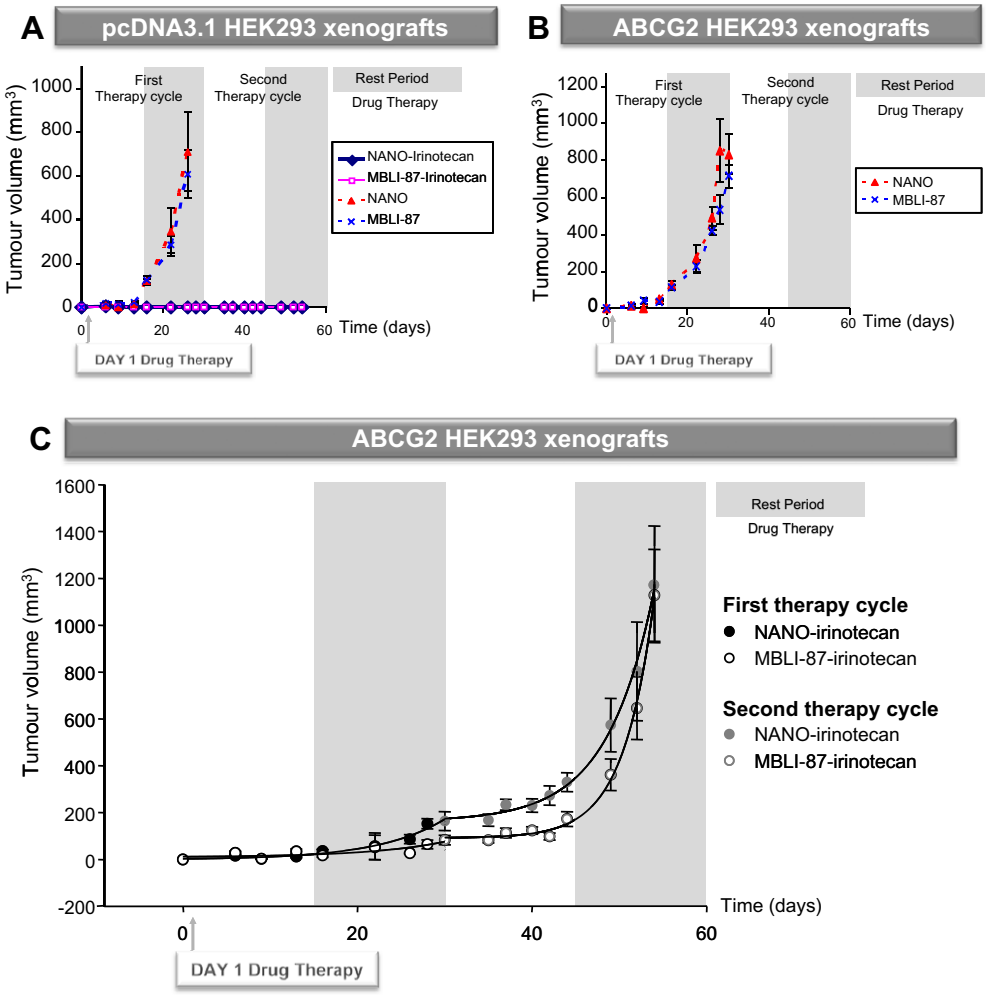

Fig. 3 – Activity of MBLI-87, NANO and irinotecan, either alone or in combination, against control (A) and ABCG2-expressing (B and C) xenografts. Doses and schedules are detailed in Section 2. (A and B) The data at each time period were averaged. The tumour volume values were plotted against time. Differences with p values <0.05 were considered as statistically significant between two sets of xenograft volume (N = 6/group). (C) Mice were treated with either NANO or MBLI-87 in combination with irinotecan. The data were sets of tumour measurements (in sixes) at four time periods: first therapy period, first rest period, second therapy period and second rest period, for two parallel therapy conditions: MBLI-87-irinotecan (N = 5) and NANO-irinotecan (N = 6). The data at each time period were averaged and standard errors (SE) computed. A plot was made of tumour volume ± SE against time.

therapy period likely potentiated drug effects on the implanted cells, through a direct action on the cells. In contrast, the second drug therapy period (from day 30 to 44) was performed when xenograft volumes were in the mean range of 100 mm^3, an established tumour size. Although some concentration variability was observed, both SN-38 and irinotecan were detected in xenografts, by LC–MS/MS, 24 h after irinotecan administration. Control xenografts, treated with NANO, grew and reached a maximal volume at day 28, whereas they did not grow at all during the 8-week period following irinotecan therapy (Fig. 3A). NANO-irinotecan and MBLI-87-irinotecan therapies completely prevented the growth of control xenografts during the first 8 weeks (Fig. 3A). MBLI-87 alone did not significantly modify the growth of either pcDNA3.1- or ABCG2-xenografts when compared to control NANO (Fig. 3A and B). Compared to its effect on the pcDNA3.1 control xenografts, treatment with irinotecan alone delayed the growth of ABCG2-expressing xenografts by approximately 10 days (Fig. 3C *versus* B).

We observed an inhibition by MBLI-87 of ABCG2-dependent resistance to irinotecan during the second chemotherapy cycle, examining the day 30–54 period (Fig. 3C). ABCG2 tumour growth was delayed by co-administration of MBLI-87 and irinotecan, in comparison to NANO and irinotecan during the first rest period and the second therapy period. The data points of the overall MBLI-87 series were significantly below those of the NANO series (Paired t-test, $p < 0.001$). This was especially true over the time period of 35–54 days.

To further evaluate the difference between the two treatments, a kinetic analysis was performed. The points depicted in Fig. 3C were better fitted (F test, at $p < 0.01$) for both test and

Table 1 – Parameters of MBLI-87-irinotecan and NANO-irinotecan exponential growth equations[a].

	Coefficient	Std. error		P-value
NANO-irinotecan (0–30 days)				
$R^2 = 0.9702$		$f = -0.6424 + 3.2693 * \exp(0.1322 * x)$		
y_0	−0.6424	10.2939	ns	0.9523
a	3.2693	2.9354	ns	0.308
b	0.1322	0.0294	*	0.0041
MBLI-87-irinotecan (0–30 days)				
$R^2 = 0.7293$		$f = 9.7198 + 2.0402 * \exp(0.1162 * x)$		
y_0	9.7198	16.1066	ns	0.5683
a	2.0402	6.0361	ns	0.7469
b	0.1162	0.0954	ns	0.2691
NANO-irinotecan (30–54 days)				
$R^2 = 0.9954$		$f = 163.1692 + 0.0437 * \exp(0.1857 * x)$		
y_0	163.1692	19.6266	**	0.0002
a	0.0437	0.0361	ns	0.2709
b	0.1857	0.0152	***	<0.0001
MBLI-87-irinotecan (30–54 days)				
$R^2 = 0.9969$		$f = 91.6966 + 0.0002 * \exp(0.2836 * x)$		
y_0	91.6966	11.4804	**	0.0002
a	0.0002	0.0002	ns	0.3233
b	0.2836	0.0173	***	<0.0001

* $p < 0.01$.
** $p < 0.001$.
*** $p < 0.0001$.
[a] The points of the Fig. 3C were better fitted (F test, at $p < 0.01$) for both test and control series, as two separate (rather than a single one) time courses following the augmented (three parameter) exponential growth equation: $y = y_0 + a * \exp(b * t)$, where $y_0 + 1$ is the computed size at $t = 0$, a is 1.71828 times the increment in size at time equal to $1/b$, whilst b is the growth rate constant. The p values reflect the goodness of fit of the growth rate equation to the data, and not the comparison between the two treatments. The two treatments were not statistically different when compared for the period from 0 to 30 days ($p = 0.115$), but they were indeed statistically different when compared for the period from 30 to 54 days ($p < 0.001$).

control series, as two separate (rather than a single one) time courses following the augmented (three-parameter) exponential growth equation: $y = y_0 + a * \exp(b * t)$, where $y_0 + 1$ is the computed size at $t = 0$, a is 1.71828 times the increment in size at times equal to $1/b$, whilst b is the growth rate constant (Table 1). Although there was no statistically-supported difference ($p = 0.115$) for the whole 0–30 day period, a statistically significant difference was indeed observed over the first rest period (day 16–30), $p = 0.039$.

The growth rate during the second drug therapy period (day 30–44) appeared to be slower for MBLI-87-irinotecan than for NANO-irinotecan although this did not reach statistically significance ($p = 0.883$). Surprisingly, following discontinuation of therapy, growth of the tumours accelerated, and more so for the MBLI-87-irinotecan group. Growth started from a lower point and yet reached the same end size. For the statistical analysis of the entire growth period (comprising the second drug therapy and rest combined (day 30–54)), there were enough data points to give a satisfactory p value ($p < 0.001$) for the difference in the growth rate constants: b (NANO-irinotecan) − b (MBLI-87-irinotecan) = 0.1857 − 0.2836 = −0.0979; $t = -4.251$ with 16 degrees of freedom ($P < 0.001$), and 95 percent confidence interval for difference of means: −0.147 to −0.0491 (the power of performed test with $\alpha = 0.050$:0.981). Thus, the growth rate constant (b) in the MBLI-87-irinotecan case was 50% higher than that in NANO-irinotecan and this was supported at $p < 0.001$ (Table 1). A possible explanation is that the growth rate of the xenograft accelerates when treatment with MBLI-87-irinotecan is discontinued. A similar phenomenon was observed for tumour growth in humans upon cessation of treatment with bevacizumab (Avastin),[22] also suggesting a tumour growth acceleration after drug removal and hence an apparently similar phenomenon in our animal model. Regardless of whether the tumour accelerates or simply returns to a pre-treatment growth rate, this model may have relevance for the clinical situation, showing that we cannot expect a "permanent" benefit after discontinuation of therapy.

MBLI-87 was selected as a specific, non-toxic inhibitor of ABCG2, not interacting with ABCB1. MBLI-87 could not be experimentally assayed at a maximum tolerable dose, due to limited solubility. It was not toxic for mice, its usable dose being here limited by the maximal volume that could be injected (300 μL). Furthermore, since ABCG2 is physiologically expressed in various tissues (liver, BHE and intestine), we evaluated the influence of MBLI-87 on SN-38 and irinotecan in plasma in pharmacokinetic experiments. Irinotecan disposition was evaluated in tumour-free mice after a single IP injection of irinotecan (20 mg/kg) with either MBLI-87 (3.45 mg/kg) or the NANO vehicle control. Under our conditions, irinotecan concentrations followed a two-phase decay (Fig. 4A); they were high at 30 min, decreased strongly after 3 h exposure and remained detectable after 24 h. We also quantified SN-38, the active metabolite of irinotecan, in plasma. Interestingly, with a slight delay likely due to metabolism kinetics, the high concentration of SN-38 was reached at the 3 h timepoint and decreased strongly but remained still detectable 24 h after injection (Fig. 4B). The median values per timepoint and the AUCs (AUC (NANO-irinotecan) = 20117.76 ng/mL/h ± 13356.18 (SD); AUC (MBLI-87-irinotecan) = 18160.34 ng/mL/h ± 2855.506 (SD); AUC (SN-38-NANO) = 3712.245 ng/mL/h ± 767.17 (SD); AUC (SN-38-MBLI-87) = 3242.69 ng/mL/h ± 856.8481 (SD)) were similar for the different conditions. Consequently, MBLI-87 had no effect on SN-38 and irinotecan concentrations and, presumably, on their related toxicity. Such a lack of interference of MBLI-87 towards irinotecan and SN-38 disposition encourages further studies.

The results presented above show evident sensitisation to therapy by MBLI-87 at earlier timepoints, which at later timepoints is negated by the acceleration of tumour growth that occurs following discontinuation of therapy. We consider that these studies serve as proof of concept and suggest that optimisation of both the injectable MBLI-87 preparation and its *in vivo* therapeutic protocol is a worthwhile endeavour, toward preclinical modelling of ABCG2 inhibition. If MBLI-87 is indeed confirmed as a potent non-toxic inhibitor towards other drugs and in other model systems, it will constitute a good candidate for further development aimed at improving bioavailability of substrate drugs, CNS penetration, accumulation of targeted agents in stem cells and possibly to overcome multidrug resistance in cancer.

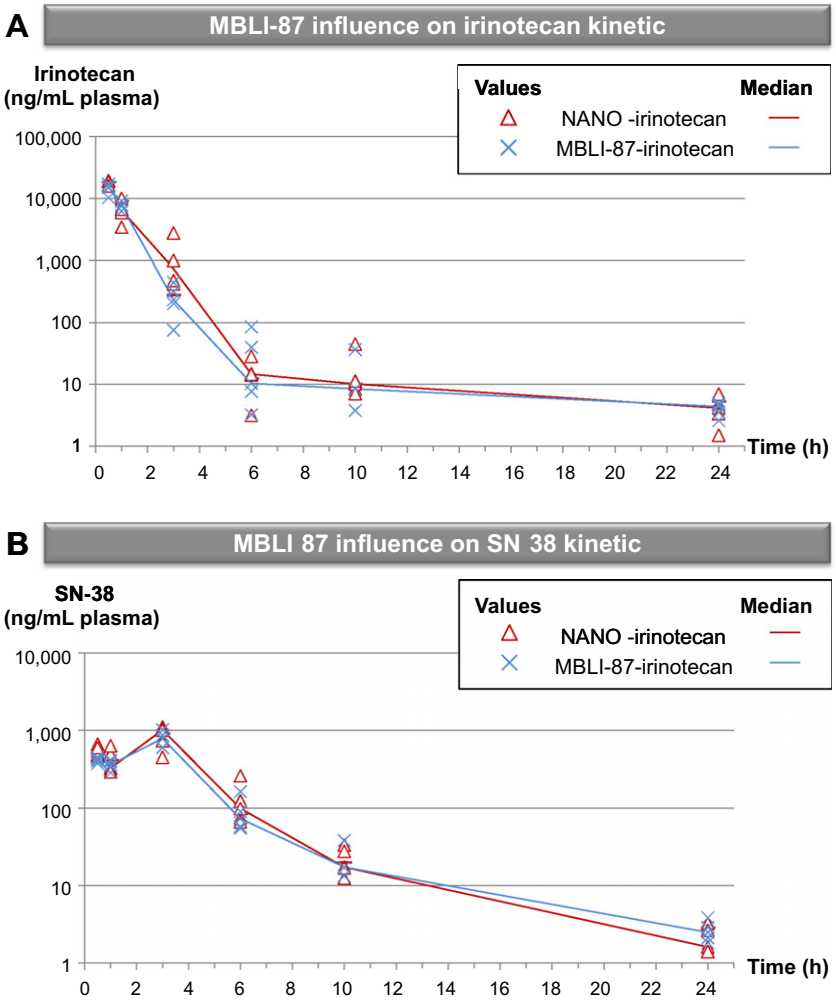

Fig. 4 – Representative plots of irinotecan (A) and SN-38 (B) plasma concentrations as a function of time. Mice were treated by IP injection of irinotecan in combination with either MBLI-87 or NANO (5 mice per condition). HPLC MS/MS determined irinotecan and SN-38 plasma concentrations (ng/mL plasma) are represented as plots as a function of time. Irinotecan (A) or SN-38 (B) plasma concentration of each mouse is shown in the absence (red triangles/NANO-irinotecan) or presence of MBLI-87 (blue crosses/MBLI-87-irinotecan). Median values are either represented by a red line (NANO-irinotecan) or a blue line (MBLI-87-irinotecan). (For interpretation of the references to colour in this figure legend, the reader is referred to the web version of this article.)

Conflict interest statement

None declared.

Acknowledgements

This work was supported by INSERM (UMR 590) and Université Lyon 1, and grants from Association pour la Recherche sur le Cancer (ARC 4007), Ligue Nationale contre le Cancer (Equipe labellisée Ligue 2009) and LST (Lyon Science Transfert). M. Honorat and O. Arnaud are respectively recipient of doctoral fellowships from the Ligue Nationale contre le Cancer and the Ministère de l'Enseignement Supérieur et de la Recherche.

REFERENCES

1. Shukla S, Zaher H, Hartz A, et al. Curcumin inhibits the activity of ABCG2/BCRP1, a multidrug resistance-linked ABC drug transporter in mice. *Pharm Res* 2009;**26**(2):480–7.
2. Deeken JF, Figg WD, Bates SE, Sparreboom A. Toward individualized treatment: prediction of anticancer drug disposition and toxicity with pharmacogenetics. *Anticancer Drugs* 2007;**18**(2):111–26.
3. Loscher W, Potschka H. Blood–brain barrier active efflux transporters: ATP-binding cassette gene family. *NeuroRx* 2005;**2**(1):86–98.
4. Polli JW, Olson KL, Chism JP, et al. An unexpected synergist role of P-glycoprotein and breast cancer resistance protein on the central nervous system penetration of the tyrosine kinase inhibitor lapatinib (N-{3-chloro-4-[(3-fluorobenzyl)oxy]phenyl}-6-[5-({[2-(methylsulfonyl)ethy

l]amino}methyl)-2-furyl]-4-quinazolinamine; GW572016). *Drug Metab Dispos* 2009;**37**(2):439–42.
5. Smith NF, Figg WD, Sparreboom A. Pharmacogenetics of irinotecan metabolism and transport: an update. *Toxicol In Vitro* 2006;**20**(2):163–75.
6. Chu XY, Suzuki H, Ueda K, et al. Active efflux of CPT-11 and its metabolites in human KB-derived cell lines. *J Pharmacol Exp Ther* 1999;**288**(2):735–41.
7. Nicolle E, Boumendjel A, Macalou S, et al. QSAR analysis and molecular modeling of ABCG2-specific inhibitors. *Adv Drug Deliv Rev* 2009;**61**(1):34–46.
8. Hida T, Ogawa S, Park JC, et al. Gefitinib for the treatment of non-small-cell lung cancer. *Expert Rev Anticancer Ther* 2009;**9**(1):17–35.
9. Lemos C, Jansen G, Peters GJ. Drug transporters: recent advances concerning BCRP and tyrosine kinase inhibitors. *Br J Cancer* 2008;**98**(5):857–62.
10. Stewart CF, Leggas M, Schuetz JD, et al. Gefitinib enhances the antitumor activity and oral bioavailability of irinotecan in mice. *Cancer Res* 2004;**64**(20):7491–9.
11. Elkind NB, Szentpetery Z, Apati A, et al. Multidrug transporter ABCG2 prevents tumor cell death induced by the epidermal growth factor receptor inhibitor Iressa (ZD1839, Gefitinib). *Cancer Res* 2005;**65**(5):1770–7.
12. Leggas M, Panetta JC, Zhuang Y, et al. Gefitinib modulates the function of multiple ATP-binding cassette transporters *in vivo*. *Cancer Res* 2006;**66**(9):4802–7.
13. Yanase K, Tsukahara S, Asada S, et al. Gefitinib reverses breast cancer resistance protein-mediated drug resistance. *Mol Cancer Ther* 2004;**3**(9):1119–25.
14. Ahmed-Belkacem A, Pozza A, Munoz-Martinez F, et al. Flavonoid structure-activity studies identify 6-prenylchrysin and tectochrysin as potent and specific inhibitors of breast cancer resistance protein ABCG2. *Cancer Res* 2005;**65**(11):4852–60.
15. Boumendjel A, Macalou S, Ahmed-Belkacem A, Blanc M, Di Pietro A. Acridone derivatives: design, synthesis, and inhibition of breast cancer resistance protein ABCG2. *Bioorg Med Chem* 2007;**15**(8):2892–7.
16. Macalou S, Pozza A, Terreux R, Magnard S, Boumendjel A, Pietro AD. Discriminating selective and non-selective inhibitory sites of ABCG2 with acridone derivates. 2010, submitted for publication.
17. Robey RW, Honjo Y, Morisaki K, et al. Mutations at amino-acid 482 in the ABCG2 gene affect substrate and antagonist specificity. *Br J Cancer* 2003;**89**(10):1971–8.
18. Choisnard L, Geze A, Putaux JL, Wong YS, Wouessidjewe D. Nanoparticles of beta-cyclodextrin esters obtained by self-assembling of biotransesterified beta-cyclodextrins. *Biomacromolecules* 2006;**7**(2):515–20.
19. Gèze A, Choisnard L, Putaux JL, Wouessidjewe D. Colloidal systems made of biotransesterified alpha, beta and gamma cyclodextrins grafted with C10 alkyl chains. *Mater Sci Eng C* 2009;**29**:458–62.
20. Choisnard L, Geze A, Yameogo BG, Putaux JL, Wouessidjewe D. Miscellaneous nanoaggregates made of beta-CD esters synthesised by an enzymatic pathway. *Int J Pharm* 2007; **344**(1–2):26–32.
21. Zhang Y, Bressler JP, Neal J, et al. ABCG2/BCRP expression modulates D-luciferin based bioluminescence imaging. *Cancer Res* 2007;**67**(19):9389–97.
22. Stein WD, Yang J, Bates SE, Fojo T. Bevacizumab reduces the growth rate constants of renal carcinomas: a novel algorithm suggests early discontinuation of bevacizumab resulted in a lack of survival advantage. *Oncologist* 2008;**13**(10):1055–62.